Supplementary Information

Lead Free Perovskite Semiconductors Based on Germanium-Tin Solid Solutions: Structural and Optoelectronic Properties

Satyawan Nagane,[1,‡] Dibyajyoti Ghosh,[2,‡] Robert L. Z. Hoye,[3] Baodan Zhao,[3] Shahab Ahmad,[4] Alison B. Walker,[2] M. Saiful Islam,[5] Satishchandra Ogale[1*] and Aditya Sadhanala[3*]*

[1]Department of Physics and Centre for Energy Science, Indian Institute of Science Education and Research (IISER), Dr. Homi Bhabha Road, Pune 411 008, India.

[2]Department of Physics, University of Bath, Bath BA2 7AY, United Kingdom.

[3]Cavendish Laboratory, University of Cambridge, JJ Thomson Avenue, CB3 0HE, Cambridge, United Kingdom.

[4]Institute for Manufacturing, Department of Engineering, University of Cambridge, 17 Charles Babbage Road, Cambridge CB3 0FS, United Kingdom.

[5]Department of Chemistry, University of Bath, Bath BA2 7AY, United Kingdom.

Experimental:

Materials: All materials used for synthesis were purchased from Sigma-Aldrich, Alfa-Aesar, Dye-sol and American elements. These materials were used as received without further purification.

Synthesis procedure for solution based $CH_3NH_3Sn_xGe_{1-x}I_3$ ($0 \leq X \leq 1$) perovskites: For the synthesis of these mixed metal based-perovskites, we have used well studied single step solution method.

Synthesis of $CH_3NH_3SnI_3$: SnI_2 beads (0.186 gm, 5 mmol) and CH_3NH_3I (0.079 gm, 5 mmol) was dissolved in anhydrous *N*, *N*-dimethylformamide (DMF) 1 mL (This solution was used as a stock solution for synthesis of binary metal based-perovskite). In order to get powder from the stock solution, we have poured this stock solution dropwise in chloroform (acts as anti-solvent). The black precipitate settles down at bottom which was washed (2-3 times) by chloroform to remove traces of DMF. The black precipitate was then dried by heating at 90 - 100^{o}C in argon glove box. The perovskite powder achieved by precipitation was further used for XRD and other spectroscopic characterization.

Thin films of **$CH_3NH_3SnI_3$** perovskite were coated on quartz substrate by spin coating (stock solution was used for spin coating) at 2000RPM for 60sec followed by annealing at 100^{O}C for 10 minutes in nitrogen filled glovebox.

Synthesis of $CH_3NH_3GeI_3$: GeI_2 powder (0.163 gm, 0.5 mmol) and CH_3NH_3I (0.079 gm, 0.5 mmol) was dissolved in anhydrous *N*, *N*-dimethylformamide (DMF) 1 mL (This solution was used as a stock solution for synthesis of binary metal based-perovskite). In order to get powder from the stock solution, we have poured this stock solution dropwise in chloroform (acts as anti-solvent for hybrid perovskites). The precipitate settles down at bottom which was washed (2-3 times) by chloroform to remove traces of DMF. The precipitate was then dried by heating at 90 -100^{o} C in argon glove box. The **$CH_3NH_3GeI_3$** perovskite powder achieved by the precipitation was further used for XRD and other spectroscopic characterization.

Thin films of **$CH_3NH_3GeI_3$** perovskite were coated on quartz substrate by spin coating (stock solution was used for spin coating) at 2000RPM for 60sec followed by annealing at $100^{O}C$ for 10 minutes in nitrogen filled glovebox.

For synthesis of binary metal based-perovskites, we have used stock solution mentioned in above two synthesis procedure. We have varied the volume of respective stock solution to achieve appropriate ratio of Ge and Sn content (25%, 50% and 75%).

Synthesis of $CH_3NH_3Sn_{0.75}Ge_{0.25}I_3$ perovskites:

750 µL **$CH_3NH_3SnI_3$** stock solution (0.5 mmol) was properly mixed with 250 µL **$CH_3NH_3GeI_3$** stock solution (0.5 mmol) in a glass vial. In order to get perovskite powder from the mixed stock solution, we have poured this solution dropwise in chloroform (acts as anti-solvent for hybrid perovskites). The precipitate settles down at bottom which was washed (2-3 times) by chloroform to remove traces of DMF. The precipitate was then dried by heating at 90 -100 °C in argon glove box. The **$CH_3NH_3Sn_{0.75}Ge_{0.25}I_3$** perovskite powder achieved by the precipitation was further used for XRD and other spectroscopic characterization.

For thin film coating, we used same solution which was prepared by mixing both the stock solution in a specific ratio and was spin coated at 2000RPM for 60sec followed by annealing at $100^{O}C$ for 10 minutes in nitrogen filled glovebox.

Synthesis of $CH_3NH_3Sn_{0.5}Ge_{0.5}I_3$ perovskites:

500 µL **$CH_3NH_3SnI_3$** stock solution (0.5 mmol) was properly mixed with 500 µL **$CH_3NH_3GeI_3$** stock solution (0.5 mmol) in a glass vial. In order to get perovskite powder from the mixed stock solution, we have poured this solution dropwise in chloroform (acts as anti-solvent for hybrid perovskites). The precipitate settles down at bottom which was washed (2-3 times) by chloroform to remove traces of DMF. The precipitate was then dried by heating at 90 -100 °C in argon glove box. The **$CH_3NH_3Sn_{0.5}Ge_{0.5}I_3$** perovskite powder achieved by the precipitation was further used for XRD and other spectroscopic characterization.

For thin film coating, we used same solution which was prepared by mixing both the stock solution in a specific ratio and was spin coated at 2000RPM for 60sec followed by annealing at $100^{O}C$ for 10 minutes in nitrogen filled glovebox.

Synthesis of $CH_3NH_3Sn_{0.25}Ge_{0.75}I_3$ perovskites:

250 µL **$CH_3NH_3SnI_3$** stock solution (0.5 mmol) was properly mixed with 750 µL **$CH_3NH_3GeI_3$** stock solution (0.5 mmol) in a glass vial. In order to get perovskite powder from the mixed stock solution, we have poured this solution dropwise in chloroform (acts as anti-solvent for hybrid perovskites). The precipitate settles down at bottom which was washed (2-3 times) by chloroform to remove traces of DMF. The precipitate was then dried by heating at 90 -100 °C in argon glove box. The **$CH_3NH_3Sn_{0.25}Ge_{0.75}I_3$** perovskite powder achieved by the precipitation was further used for XRD and other spectroscopic characterization.

For thin film coating, we used same solution which was prepared by mixing both the stock solution in a specific ratio and was spin coated at 2000RPM for 60sec followed by annealing at $100^{O}C$ for 10 minutes in nitrogen filled glovebox.

Preparation of perovskite Thin Films by thermal evaporation techniques.

Here, we have used one more deposition technique called thermal deposition technique to prepare thin films of Ge-Sn based-perovskites.

For the synthesis of Ge-Sn mixed perovskite, we used two step evaporations.

In first step, we evaporated the mixture of GeI_2 and SnI_2 with specific ratios (Ge content increases in perovskite systematically from 0% to 25%, 25% to 50% to 75% and 100%) in vacuum chamber with electric source. The quartz substrate were stacked above the evaporation source with maintaining appropriate distance.

In second step, the coated films of Ge-Sn halide then exposed to the vapours of CH_3NH_3I (CH_3NH_3I) in argon filled glove box for 25-30 minutes. The films of metal halides showed change in colour.

Materials characterization:

The materials have been characterized by using different techniques like:

X-ray diffraction patterns were taken using a Bruker D8 Advance powder X-ray diffractometer using a Cu Kα source (λ = 1.54 Å). The one-dimensional $\theta/2\theta$ scans of the thin films were measured with the samples contained in an air-free holder. The samples were rotated during the continuous scan measurements, which were taken from 10° to 80° 2θ, with a step size of 0.02° and dwell time of 0.4 s/step. The diffraction patterns were fit using the Pawley method using HighScore Plus. The crystallographic information files for $CH_3NH_3SnI_3$ and $CH_3NH_3GeI_3$ were obtained from Ref 1,2.

UV-Vis absorption (Hewlett-Packard 8453 UV−vis spectrometer) was used for absorption measurements, PDS was used to measure absorption in a highly sensitive way. For the measurements, a monochromatic pump light beam produced by a combination of a Light Support MKII 100 W Xenon arc source and a CVI DK240 monochromator, is shined on the sample (film on Quartz substrate), inclined perpendicular to the plane of the sample, which on absorption produces a thermal gradient near the sample surface via non-radiative relaxation induced heating. This results in a refractive index gradient in the area surrounding the sample surface. This refractive index gradient is further enhanced by immersing the sample in a deflection medium comprising of an inert liquid FC-72 Fluorinert® (3M Company) which has a high refractive index change per unit change in temperature. A fixed wavelength CW transverse laser probe beam, produced using a Qioptiq 670 nm fiber-coupled diode laser with temperature stabilizer for reduced beam pointing noise, was passed through the thermal gradient in front of the sample producing a deflection proportional to the absorbed light at that particular wavelength, which is detected by a differentially amplified quadrant photodiode and a Stanford Research SR830 lock-in amplifier combination. Scanning through different wavelengths gives us the complete absorption spectra.

Photoluminescence and Lifetime measurements were done using a home-built setup. A 500 mm SpectraPro2500i spectrograph (Princeton Instruments) and a thermoelectrically cooled PIXIS 100-F CCD camera (Princeton Instruments) used as a detector. A 407 nm pulsed diode laser was used as an excitation source. The laser was driven using DH400, PicoQuant laser controller. The lasers generate pulses with 80 ps full width at half maximum (FWHM) with available repetition rates over 2.5 to 40 MHz. The same setup was also used to measure PL

decay time using a ‘time correlated single photon counting’ setup (TCSPC). This setup comprises of a monochromator coupled with a micro channel plate photomultiplier tube (MCP-PMT from Hamamatsu - R3809U-50) and TCSPC electronics (Lifespec-pc and VTC900 PC card from Edinburgh Instruments). PLQY was measured using an integration sphere method described elsewhere. [3]

XRD fitting for binary metal based-hybrid perovskites.

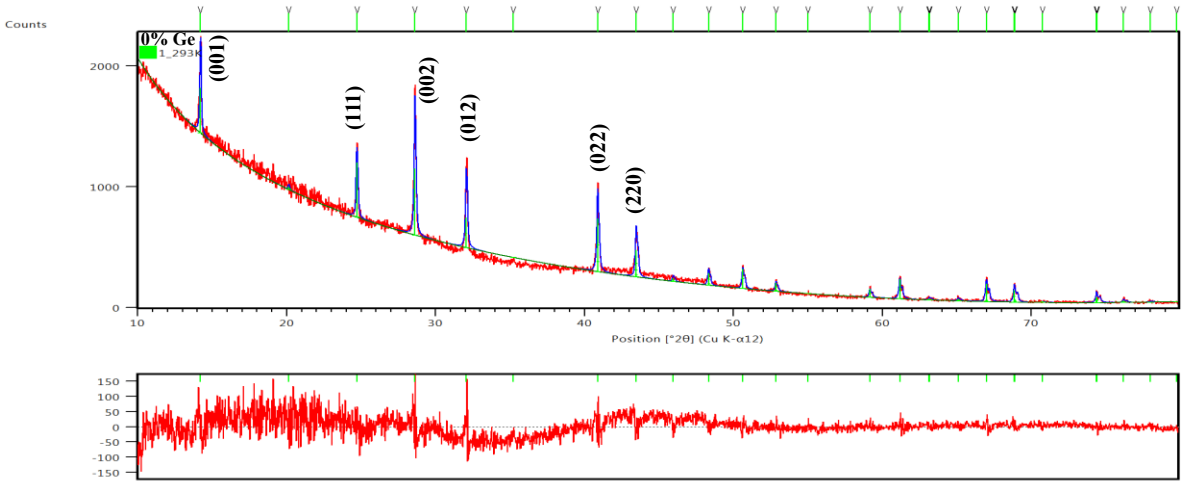

Figure S1. XRD fitting of **$CH_3NH_3SnI_3$** perovskite powder.

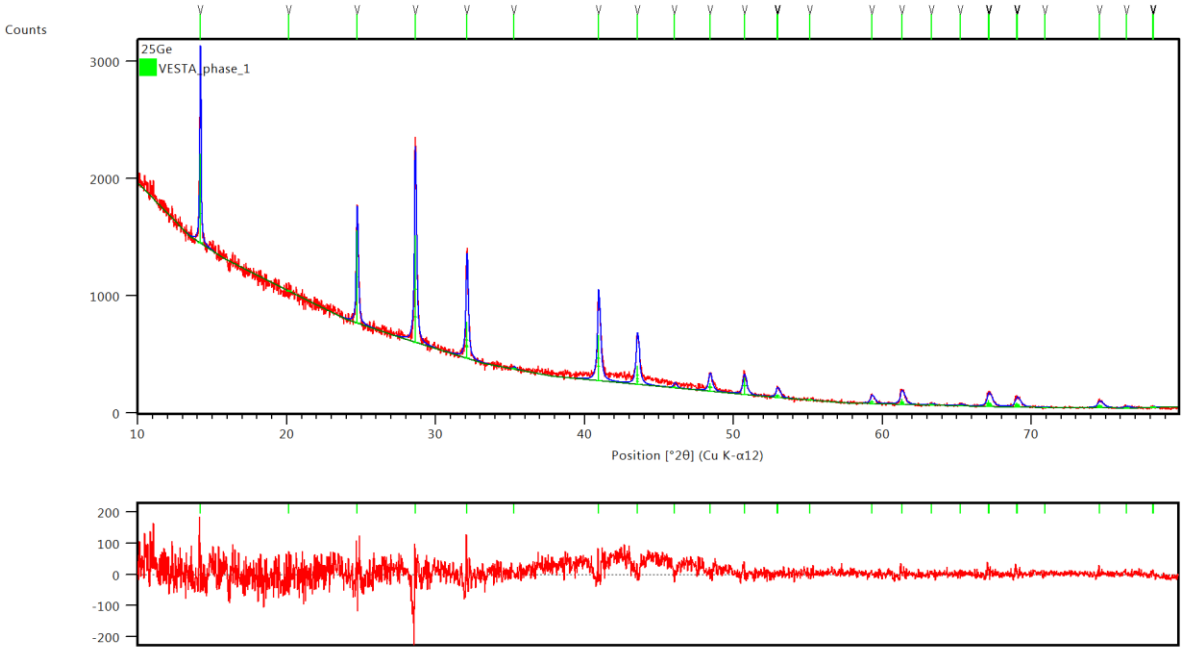

Figure S2. XRD fitting of **$CH_3NH_3Sn_{0.75}Ge_{0.25}I_3$** perovskite powder.

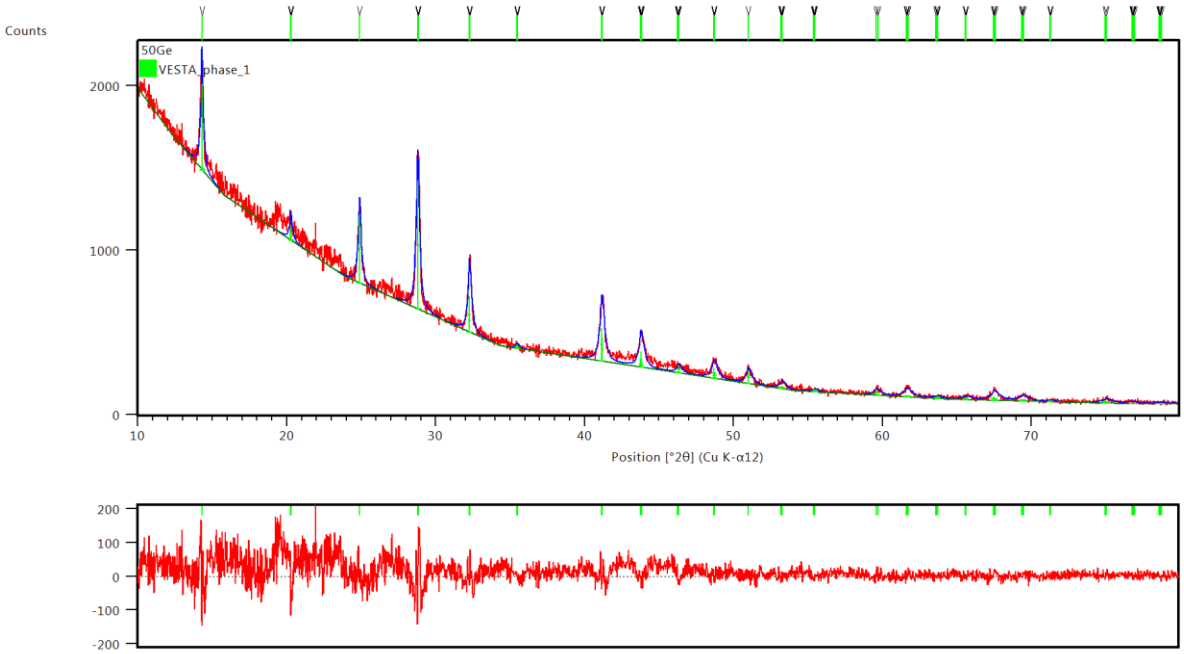

Figure S3. XRD fitting of $CH_3NH_3Sn_{0.5}Ge_{0.5}I_3$ perovskite powder.

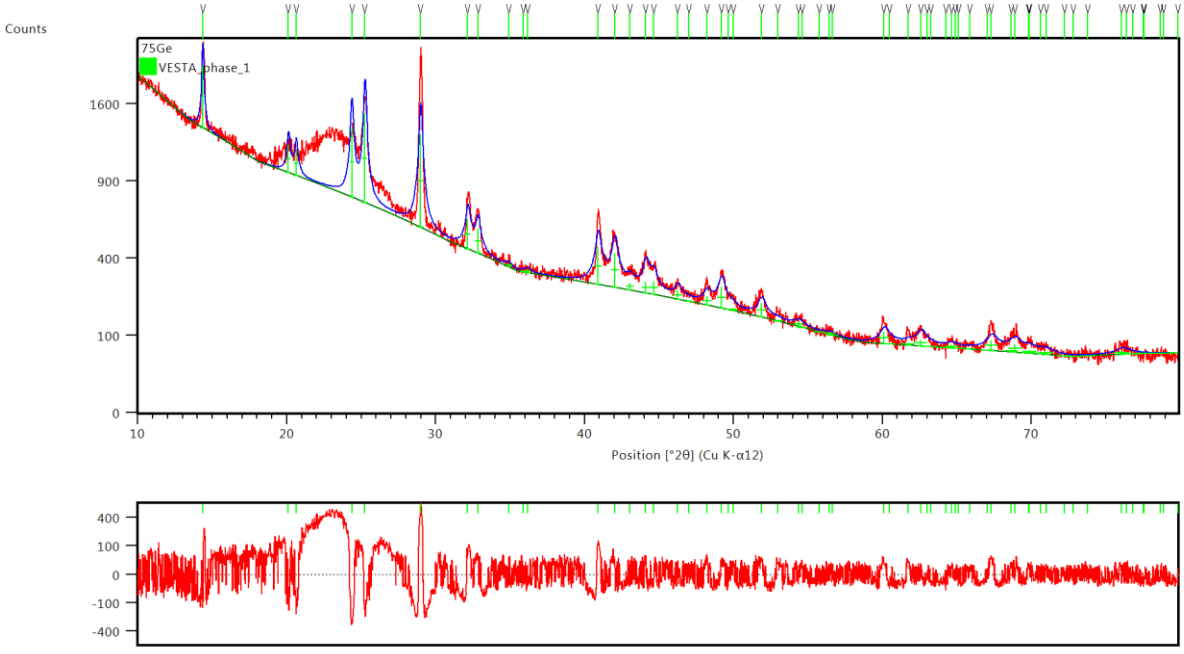

Figure S4. XRD fitting of $CH_3NH_3Sn_{0.25}Ge_{0.75}I_3$ perovskite powder.

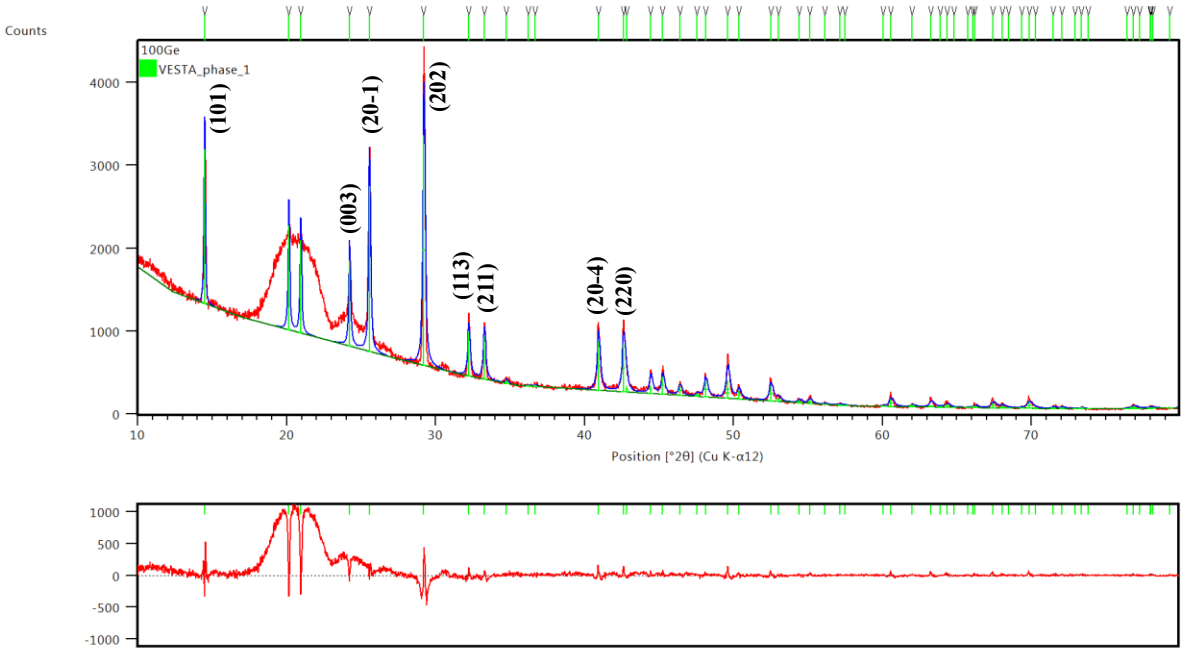

Figure S5. XRD fitting of **$CH_3NH_3GeI_3$** perovskite powder.

Table S1. Lattice parameters for $CH_3NH_3Ge_xSn_{1-x}I_3$ powder samples

Ge content (%)	Unit cell	Space group	a (A)	b (A)	c (A)	GOF (pawley)
0	Tetragonal	99	6.24	6.24	6.24	1.38
25	Tetragonal	99	6.23	6.23	6.23	1.31
50	Tetragonal	99	6.205	6.205	6.193	1.25
75	Rhombohedral	160	8.587	8.587	10.936	2.76
100	Rhombohedral	160	8.477	8.477	11.01612	5

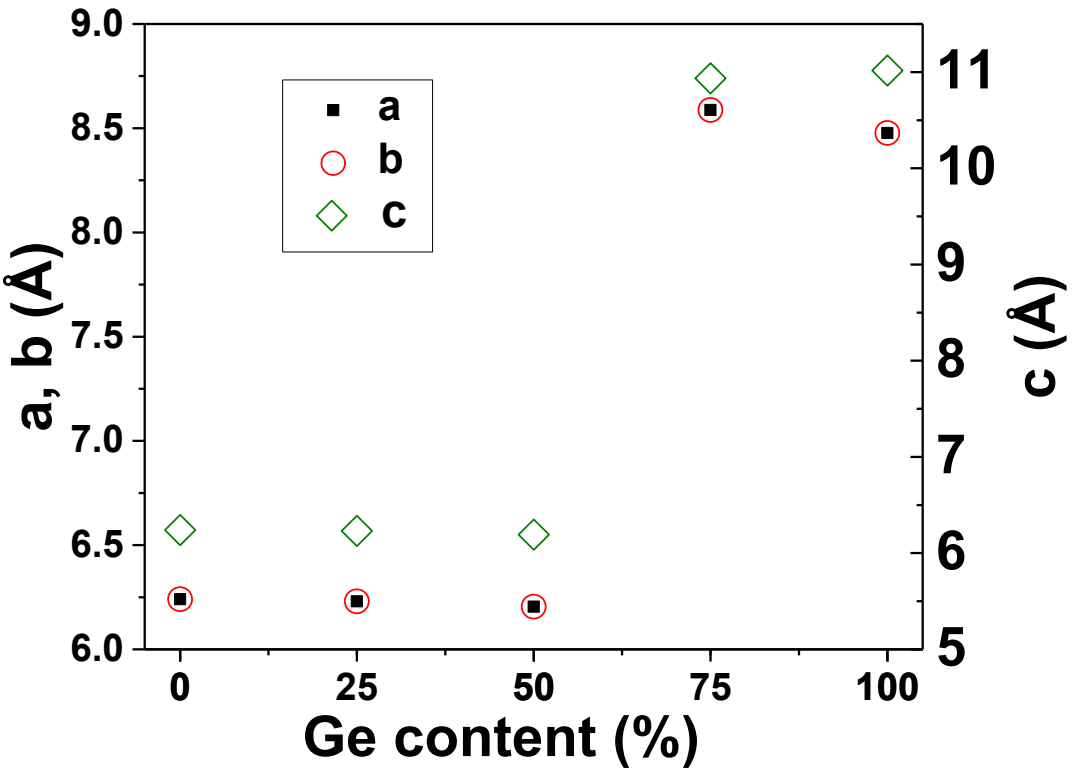

Figure S6. Figure shows the lattice parameters of $CH_3NH_3Ge_xSn_{1-x}I_3$ powder obtained from the above fits.

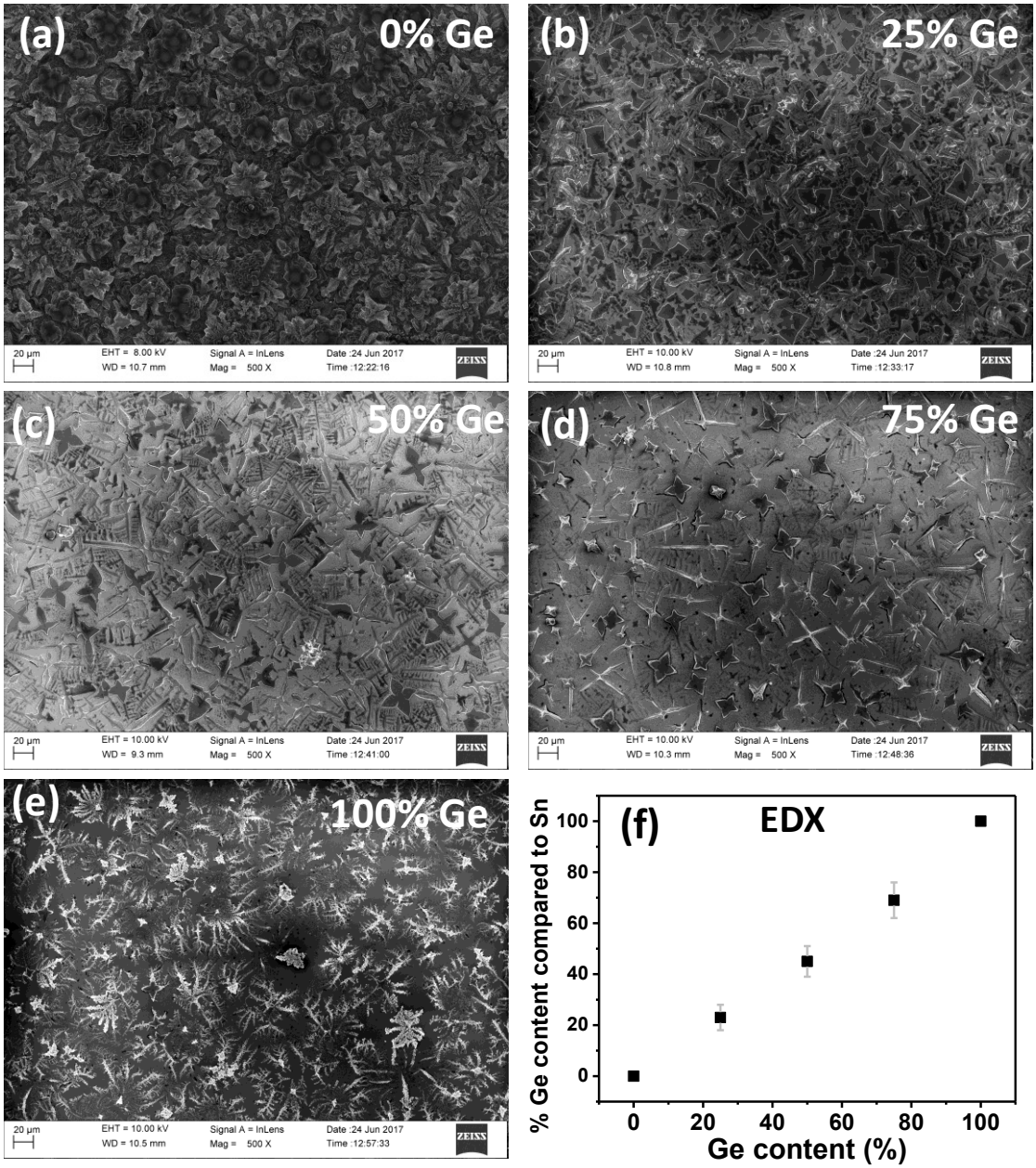

Figure S7. Microscopic (SEM) images and EDX (shows Ge content in binary metal based perovskites) of $\mathbf{CH_3NH_3Sn_xGe_{1-x}I_3}$ **(0 ≤ X ≤ 1)** perovskites.

Computational Details:

All *ab initio* calculations are performed using density functional theory (DFT) as used in previous successful studies on hybrid perovskites [4,5], and implemented in the Vienna Ab initio Simulation Package (VASP 5.3.5)[6]. In order to construct the plane-wave basis-set, a cut-off of 500 eV has been used. Ion-electron interactions are included by employing the projected augmented wave (PAW) method[7]. Generalized gradient approximations (GGA) in the form of Perdew-Burke-Ernzerhof functionals for solids (PBEsol) capture the exchange-correlation interactions[8]. Note that although GGA-PBEsol functionals underestimate the absolute band-gap of hybrid perovskites, they successfully reproduce the trend in band-gap values for similar mixed perovskites[9]. To describe the band-dispersion, spin-orbit coupling (SOC) was included for valence electrons for the band structure calculations. To calculate the conductivity effective mass within the constant relaxation time approximation, BoltzTraP code has been used [10]. We have performed ab initio molecular dynamics simulations using QUICKSTEP module of CP2K package using a large (3x3x3) supercell [11].
As indicated by experimental observations, we consider the possible decomposition pathway for these mixed metal perovskites as follows:

$$CH_3NH_3Sn_{(1-x)}Ge_xI_3 = CH_3NH_3I + (1-x)SnI_2 + xGeI_2 \quad \ldots\ldots\ldots\ldots\ldots (1)$$

The corresponding decomposition enthalpy can be formulated as,

$$\Delta H = E[CH_3NH_3Sn_{(1-x)}Ge_xI_3] - E[CH_3NH_3I] - (1-x)E[SnI_2] - xE[GeI_2] \quad \ldots\ldots\ldots\ldots\ldots\ldots (2)$$

where $E[CH_3NH_3Sn_xGe_{(1-x)}I_3]$, $E[CH_3NH_3I]$, $E[SnI_2]$ and $E[GeI_2]$ are the total energies per formula unit.

The Goldschmidt tolerance factor (t) can be formulated as,

$$t = \frac{r_A + r_X}{\sqrt{2}(r_B + r_X)} \quad \ldots\ldots\ldots\ldots\ldots\ldots\ldots\ldots\ldots\ldots\ldots\ldots\ldots\ldots\ldots\ldots\ldots\ldots (3)$$

where r_A, r_B and r_X are effective ionic radii of $CH_3NH_3^+$ cations, Sn/Ge metal atoms and I anions, respectively. Generally, a Goldschmidt tolerance factor (t) in the range $0.8 \leq t \leq 1$ indicates stable

perovskite structures.[12] Here, B sites are occupied by metal cations *i.e.* Sn and Ge. Therefore, we have used the following expression to calculate the mean effective radii of B^{2+} cations in $CH_3NH_3Sn_{(1-x)}Ge_xI_3$, $r_B = \{x \times r_{Sn2+} + (1-x) \times r_{Ge2+}\}$. The effective ionic radii of $CH_3NH_3^{+}$, Sn^{2+}, Ge^{2+} and I^- are 1.8 Å, 1.18 Å, 0.73 Å and 2.2 Å, respectively [13,14].

To optimize the geometries of $CH_3NH_3Sn_{(1-x)}Ge_xI_3$ using DFT-based calculations, the lattice parameters remained fixed to the experimentally measured values and the atomic positions were relaxed using conjugant gradient method until the maximum force on each atom becomes less than 0.03eV $Å^{-1}$. We have used a Γ-centered k-grid with more than total 500 (700) irreducible k-points to perform Brillouin-zone integrations during all the geometry optimization (self-consistent field) calculations. For PBEsol-SOC calculations, we used k-grid with more than 300 irreducible k-points.

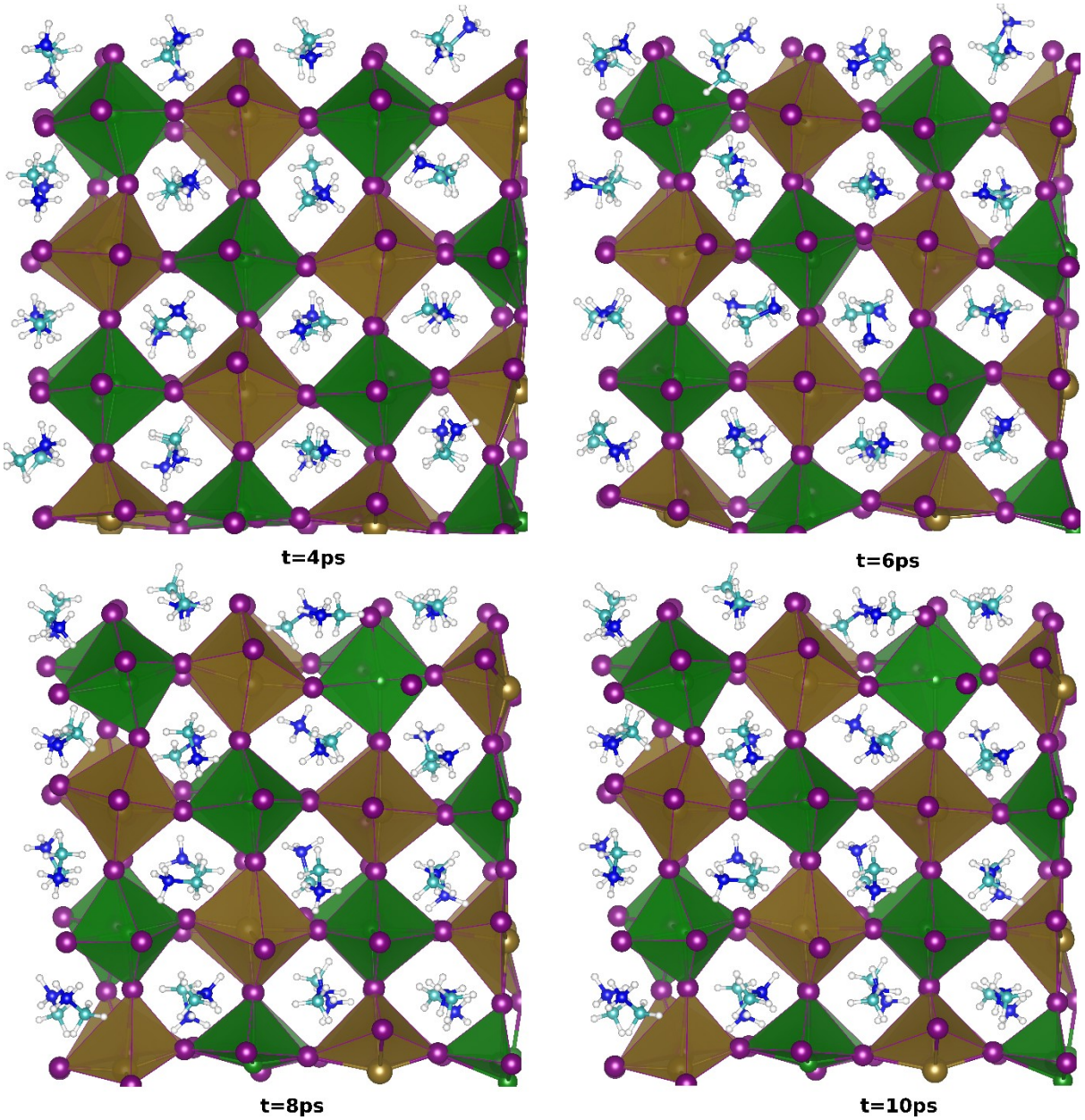

Figure S8. Snapshots of $CH_3NH_3Sn_{0.5}Ge_{0.5}I_3$ during BOMD simulation at 300K temperature. The simulation time of each frame is given at the bottom. The perovskite phase is stable after 10 ps of simulation. White, cyan, blue and pink spheres represent hydrogen, carbon, nitrogen and iodine atoms, respectively. Brown and green octahedrons represent SnI_6 and GeI_6, respectively.

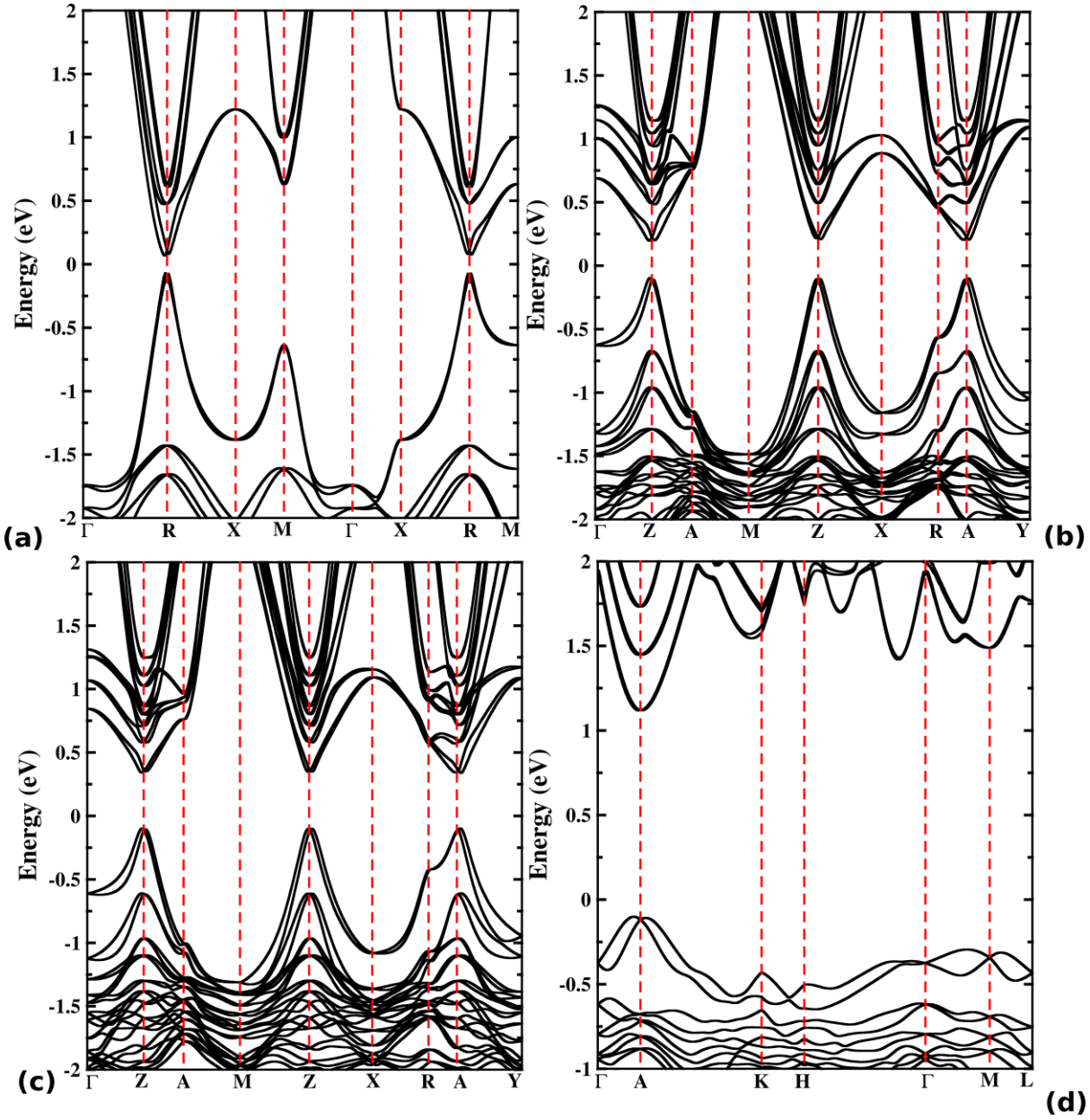

Figure S9. PBEsol+SOC calculated electronic band structures for (a) 0% Ge ($CH_3NH_3SnI_3$), (b) 25% Ge ($CH_3NH_3Sn_{0.75}Ge_{0.25}I_3$), (c) 50% Ge ($CH_3NH_3Sn_{0.5}Ge_{0.5}I_3$), (d) 100% Ge ($CH_3NH_3GeI_3$). The valence band of $CH_3NH_3GeI_3$ is much less dispersive than the other there perovskite systems shown here.

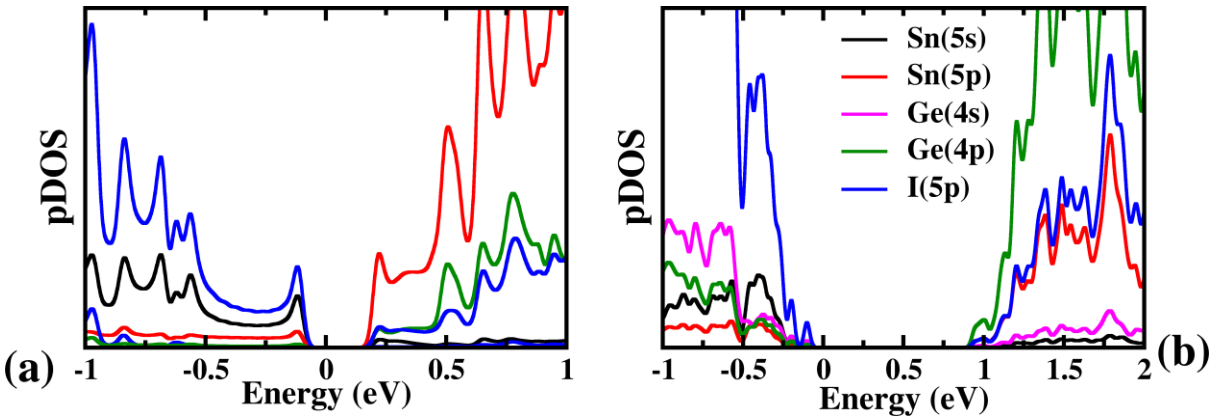

Figure S10. Projected density of states on the s and p-orbitals of Sn and Ge and 5p-orbitals of I atoms of (a) 25% Ge ($CH_3NH_3Sn_{0.25}Ge_{0.75}I_3$) and (b) 75% Ge ($CH_3NH_3Sn_{0.25}Ge_{0.75}I_3$) calculated using PBEsol-SOC.

Table S2. Optimized ranges of bond lengths of $CH_3NH_3Sn_xGe_{(1-x)}I_3$ perovskites.

System	Sn-I bond	Ge-I bond	H_N-I bond	H_C-I bond
$CH_3NH_3SnI_3$	2.99-3.13	-	2.63-2.72	3.29-3.39
$CH_3NH_3Sn_{0.75}Ge_{0.25}I_3$	3.23-3.01	2.78-3.45	2.67-2.78	3.25-3.42
$CH_3NH_3Sn_{0.5}Ge_{0.5}I_3$	3.30-3.05	2.78-3.42	2.64-2.94	3.35-3.55
$CH_3NH_3Sn_{0.25}Ge_{O.75}I_3$	2.93-3.48	2.69-3.50	2.57-2.88	2.95-3.17
$CH_3NH_3GeI_3$	-	2.7-3.5	2.58-2.87	2.85-3.12

Table S3. Calculated electronic band-gaps for $CH_3NH_3Sn_xGe_{(1-x)}I_3$ perovskites using PBEsol-SOC.

Systems	Band Gap (eV)
0% Ge ($CH_3NH_3SnI_3$)	0.14
25% Ge ($CH_3NH_3Sn_{0.75}Ge_{0.25}I_3$)	0.29
50% Ge ($CH_3NH_3Sn_{0.5}Ge_{0.5}I_3$)	0.44
75% Ge ($CH_3NH_3Sn_{0.25}Ge_{O.75}I_3$)	0.97
100% Ge ($CH_3NH_3GeI_3$)	1.15

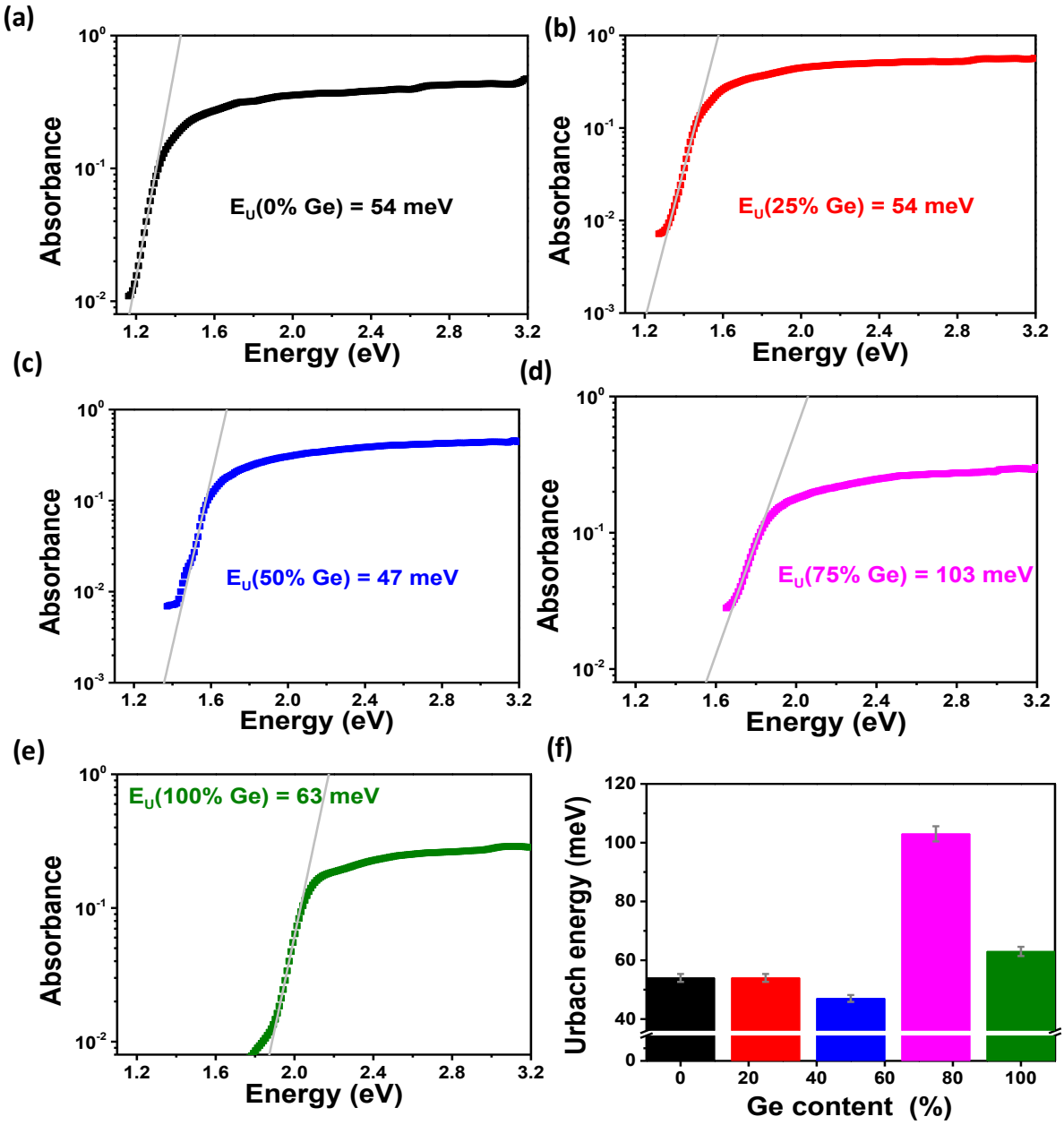

Figure S11. Fits to the PDS data to obtain Urbach energy (E_U) using the expression $A = A_0 \exp(E/E_U)$, where, A is the absorbance, A_0 is a constant and E is the energy of the photon.

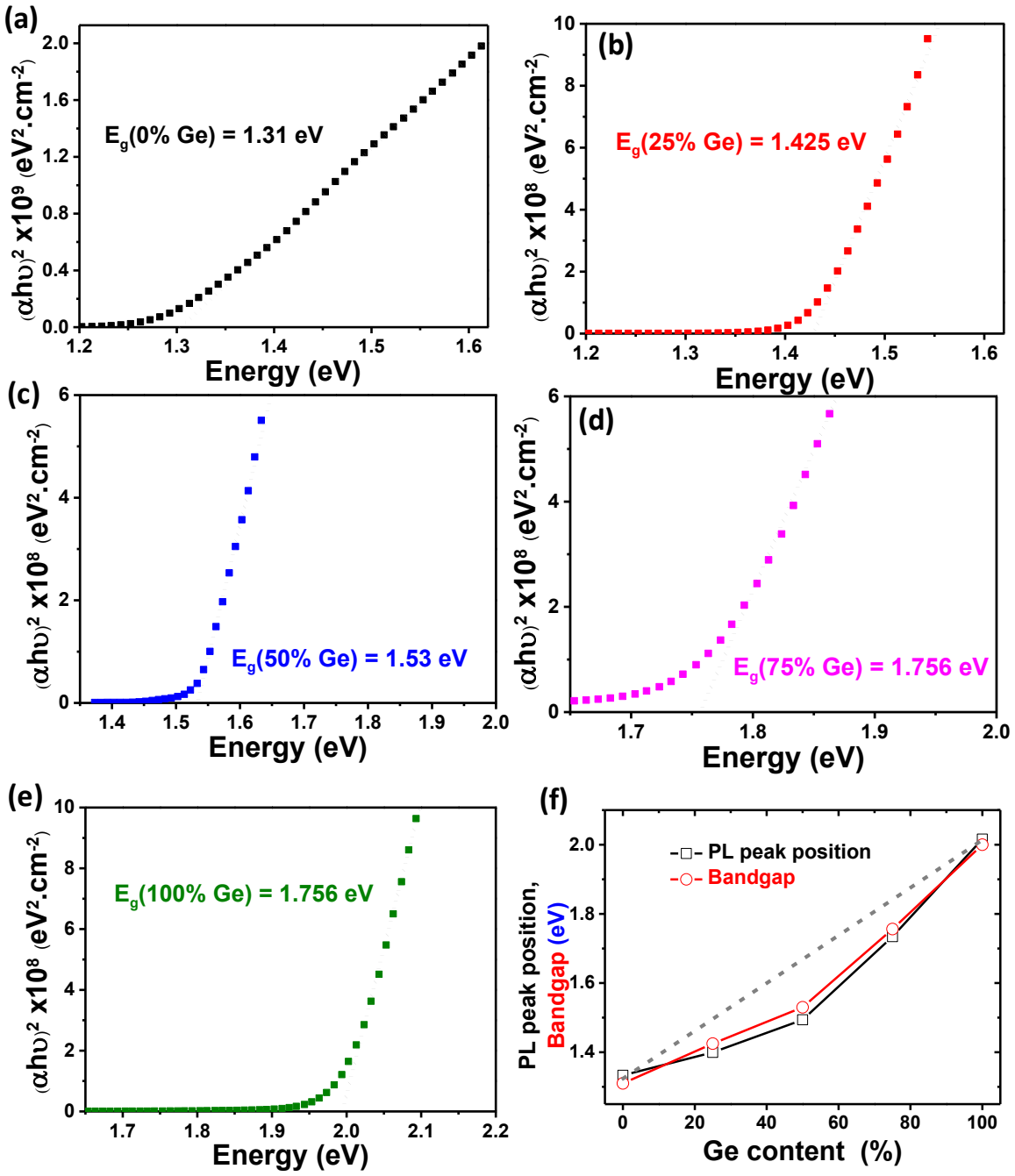

Figure S12. Fits to the absorption tail to obtain the bandgap (E_g) using direct bandgap method of Tauc plots.

References:

(1) Stoumpos, C. C.; Malliakas, C. D.; Kanatzidis, M. G. Semiconducting Tin and Lead Iodide Perovskites with Organic Cations: Phase Transitions, High Mobilities, and near-Infrared Photoluminescent Properties. *Inorg. Chem.* **2013**, *52* (15), 9019–9038.

(2) Stoumpos, C. C.; Frazer, L.; Clark, D. J.; Kim, Y. S.; Rhim, S. H.; Freeman, A. J.; Ketterson, J. B.; Jang, J. I.; Kanatzidis, M. G. Hybrid Germanium Iodide Perovskite Semiconductors:

Active Lone Pairs, Structural Distortions, Direct and Indirect Energy Gaps, and Strong Nonlinear Optical Properties. *J. Am. Chem. Soc.* **2015**, *137* (21), 6804–6819.

(3) de Mello, J. C.; Wittmann, H. F.; Friend, R. H. An Improved Experimental Determination of External Photoluminescence Quantum Efficiency. *Adv. Mater.* **1997**, *9* (3), 230–232.

(4) Aristidou, N.; Eames, C.; Sanchez-Molina, I.; Bu, X.; Kosco, J.; Islam, M. S.; Haque, S. A. Fast Oxygen Diffusion and Iodide Defects Mediate Oxygen-Induced Degradation of Perovskite Solar Cells. *Nat. Commun.* **2017**, *8*, 15218.

(5) Eames, C.; Frost, J. M.; Barnes, P. R. F.; O'Regan, B. C.; Walsh, A.; Islam, M. S. Ionic Transport in Hybrid Lead Iodide Perovskite Solar Cells. *Nat. Commun.* **2015**, *6*, 7497.

(6) Kresse, G.; Furthmüller, J. Efficient Iterative Schemes for *Ab Initio* Total-Energy Calculations Using a Plane-Wave Basis Set. *Phys. Rev. B* **1996**, *54* (16), 11169–11186.

(7) Kresse, G.; Joubert, D. From Ultrasoft Pseudopotentials to the Projector Augmented-Wave Method. *Phys. Rev. B* **1999**, *59* (3), 1758–1775.

(8) Perdew, J. P.; Ruzsinszky, A.; Csonka, G. I.; Vydrov, O. A.; Scuseria, G. E.; Constantin, L. A.; Zhou, X.; Burke, K. Restoring the Density-Gradient Expansion for Exchange in Solids and Surfaces. *Phys. Rev. Lett.* **2008**, *100* (13), 136406.

(9) Jung, Y.-K.; Lee, J.-H.; Walsh, A.; Soon, A. Influence of Rb/Cs Cation-Exchange on Inorganic Sn Halide Perovskites: From Chemical Structure to Physical Properties. *Chem. Mater.* **2017**, *29* (7), 3181–3188.

(10) Madsen, G. K. H.; Singh, D. J. BoltzTraP. A Code for Calculating Band-Structure Dependent Quantities. *Comput. Phys. Commun.* **2006**, *175* (1), 67–71.

(11) Hutter, J.; Iannuzzi, M.; Schiffmann, F.; VandeVondele, J. cp2k: Atomistic Simulations of Condensed Matter Systems. *Wiley Interdiscip. Rev. Comput. Mol. Sci.* **2014**, *4* (1), 15–25.

(12) Goldschmidt, V. M. Die Gesetze Der Krystallochemie. *Naturwissenschaften* **1926**, *14* (21), 477–485.

(13) Sun, P.-P.; Li, Q.-S.; Yang, L.-N.; Li, Z.-S. Theoretical Insights into a Potential Lead-Free Hybrid Perovskite: Substituting Pb 2+ with Ge 2+. *Nanoscale* **2016**, *8* (3), 1503–1512.

(14) Yoder, C. H. *Ionic Compounds*; John Wiley & Sons, Inc.: Hoboken, NJ, USA, 2006.